ON THE GAGE FACTOR FOR OPTICAL FIBER GRATING STRAIN GAGES

Richard J. Black[1], David Zare[1], Levy Oblea[1], Yong-Lae Park[1], Behzad Moslehi[1], and Craig Neslen[2]

[1]Intelligent Fiber Optic Systems Corporation (IFOS)

2363 Calle Del Mundo, Santa Clara, CA 95054-1008

[2]AFRL/RXLP, 2230 10th Street Building 655, Wright Patterson AFB, OH 45433-7817

ABSTRACT

Fiber Bragg Gratings (FBGs) can act as highly-accurate, multiplexable, EMI-immune strain gages. We provide experimental and theoretical results showing how their gage factors can vary from the well-known value of 1.2 pm per microstrain at 1550-nm wavelength for a range of grating and fiber types.

KEY WORDS: Fiber-Optic Gratings, Fiber-Optic Sensors, Strain Gage Factor

1. INTRODUCTION

Highly precise, multiplexable and electromagnetic interference immune, optical fiber grating strain gages can be key elements in structural health monitoring systems (1, 2). Measurement is based on grating wavelength changing linearly with strain. The gage factor for standard short-period fiber Bragg grating (FBG) strain gages fabricated in standard 125-micron silica fiber with Bragg wavelength at 1550 nm is well known to be 1.21 picometers of wavelength shift per microstrain applied to the fiber. However, this can differ for non standard gratings and non standard fibers. For example, long-period gratings (LPGs) can have gage factors over an order of magnitude larger than short-period gratings (SPGs). Short period FBGs in smaller diameter "bend-resistant" fibers undergo considerably more wavelength shift per unit force applied but only differ very slightly in the wavelength shift per unit strain. This paper discusses the dependence of the gage factor and related parameters on fiber and grating parameters, and applications of tailored gage factors.

This paper is structured as follows: In Section 2, we provide some theoretical background. Then, in Section 3, we discuss measurement methods followed by the experimental tests and results in Section 4, before concluding in Section 5.

2. THEORETICAL BACKGROUND

Consider an FBG fabricated with longitudinal pitch Λ between Bragg planes in an optical fiber with cladding refractive index n, modal effective index $n_{eff} = n\,(1+\Delta b)$, fractional core-cladding index difference Δ (typically <0.5%), and normalized modal parameter b ($0<b<1$). The lowest order Bragg resonance for modal reflection occurs around wavelengths $\lambda_B = 2\, n_{eff}\, \Lambda$, and the strain-induced Bragg resonance shift may then be derived as

$$(1/\lambda_B)\, d\lambda_B/d\varepsilon = (1/ n_{eff})\partial n_{eff}/\partial\varepsilon + (1/\Lambda)\partial n_{eff}/\partial\Lambda \quad (1a)$$

$$\approx (1 - p_\varepsilon),\ \varepsilon << 1,\ \Delta b << 1, \quad (1b)$$

$$\delta\lambda_B/\lambda_B \approx (1 - p_\varepsilon)\varepsilon,\ \varepsilon << 1,\ \Delta b << 1, \quad (1c)$$

where p_e is the photo-elastic coefficient of the fiber. For most silica optical fibers, we assume that the effect of core doping (typically with germanium) is negligible, and thus, taking the commonly quoted photo-elastic coefficient value in the literature for fused silica of $p_e \approx 0.22$, we have

$$\delta\lambda_B/\lambda_B \approx 0.78\ \varepsilon, \quad \varepsilon << 1,\ \Delta b << 1. \quad (1d)$$

2.1 Relation between Applied Force and Strain for Silica Fibers

When a fiber is stretched, the tensile strain ε is related to applied force F via the Young's modulus E and the cross-sectional area A, i.e.,

$$\varepsilon = F / (E_{silica}\, A_{fiber}) \quad (2)$$

An extensive literature search, including Refs. (5)-(8) among others, gave an average value of:

$$E_{silica} \approx (72.9 \pm 1.6)\ \text{Gpa} \approx (7.29 \pm 1.6) \times 10^{10}\ \text{N.m}^{-2},\ \varepsilon << 1, \quad (3)$$

Assuming this value for a 125-μm fiber gives:

$$\varepsilon / F = 1/ (E_{silica}\, A_{fiber}) \approx 0.112\%\ /\ \text{N} = 1.12\ \mu\varepsilon/ (\text{gram.m.s}^{-2}). \quad (4)$$

Taking $F = m.g = (9.81\ \text{m.s}^{-2})\ m$, where m is the mass attached to the fiber,

$$\varepsilon / m \approx\ 11.0\ \mu\varepsilon/\text{gram}. \quad (5)$$

2.2 Relation between Wavelength Shift and Force, Weight or Strain

Assuming the photelastic coefficient and approximations of Eq. 1d as well as the Young's Modulus of Eqn. 3 and thus Eq. 4, for 125-μm cladding diameter silica optical fiber, we obtain

$$(\delta\lambda_B/\lambda_B)/F \approx 0.087\ \%\ /\ \text{N}. \quad (6)$$

Then, from Eq. 5, the fractional wavelength shift per unit mass in parts-per-million (ppm) per gram is

$$(\delta\lambda_B/\lambda_B)/m \approx 8.57\ \text{ppm}\ /\ \text{gram}. \quad (7)$$

At 1300 nm

$$\delta\lambda_B /F \approx 1.13\ \text{nm}\ /\ \text{N},\ \delta\lambda_B /\delta\varepsilon\ \approx 1.01\ \text{pm}/\mu\varepsilon,\ \text{and}\ \delta\lambda_B /m \approx 11.1\ \text{pm/gram} \quad (8)$$

At 1550 nm

$$\delta\lambda_B /F \approx 1.35\ \text{nm}\ /\ \text{N},\ \delta\lambda_B /\delta\varepsilon\ \approx 1.21\ \text{pm}/\mu\varepsilon,\ \text{and}\ \delta\lambda_B /m \approx 13.3\ \text{pm/gram} \quad (9)$$

Table 1. Summary of Calculated Values assuming E_{silica} = 73 GPa, g = 9.81 ms^{-2}, $p_e \approx$ 0.22 and fiber diameter 125 □m.

λ_B [nm]	$(\delta\lambda_B / \lambda_B)/F$ [%/N]	$(\delta\lambda_B / \lambda_B)/m$ [ppm/gram]	$\delta\lambda_B / F$ [nm/N]	$\delta\lambda_B / \delta\varepsilon$ [pm/με]	$\delta\lambda_B / m$ [pm/gram]
1300	0.087	8.57	1.13	1.01	11.1
1550	0.087	8.57	1.35	1.21	13.3

3. MEASUREMENT METHODS

3.1 Hanging Weights Measurement

This method is an indirect calibrated strain test that uses weight-induced tensile strain. It first determines wavelength shift versus weight. Then, if we assume a known value of Young's modulus for the fiber, wavelength shift versus strain can be determined. In particular, as shown in Figure 1, the fiber is suspended over a pulley with a grating between the pulley and a clamp holding weights.

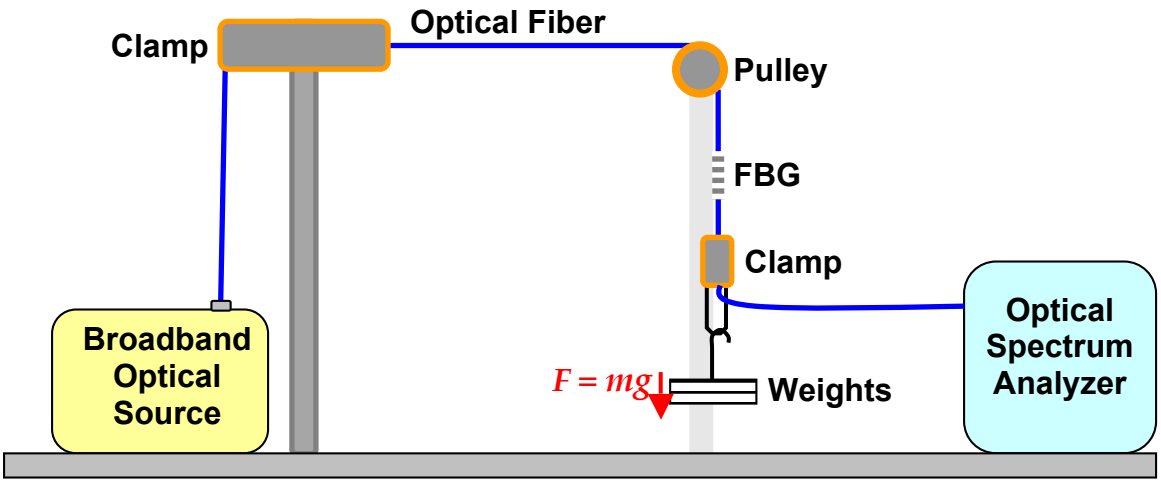

Figure 1. Hanging Weights Measurement Setup for calibrated strain tests involving providing tension on the fiber gratings with hanging weights.

3.2 Stretching Measurement

This is a direct method for measuring wavelength shift versus tensile strain. As shown in Figure 2, the grating is clamped at two points separated by a distance l. Then it is stretched by amounts δl using a precision translation stage while the Bragg wavelength is measured using a precision optical spectrum analyzer.

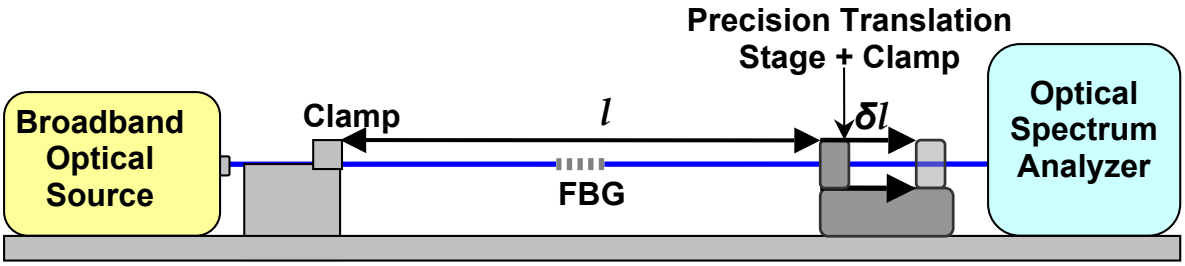

Figure 2. Stretching Measurement Setup for calibrated strain tests involving putting tensile strain $\varepsilon = \delta l/l$ on the fiber gratings via stretching an amount δl given initial length l. *The length δl is greatly exaggerated in the schematic – in general it ranges from ppm to less than 0.5%.*

4. EXPERIMENTAL RESULTS

In this section, we consider measurements of a range of fibers performed as a function of weight (force) and of strain (fractional elongation).

4.1 Standard UV Written FBGs in 125-um Cladding Single-Mode Optical Fiber

Figure 3 shows the wavelength as a function of the mass of hanging weights using the setup described in Section 3.1 (Figure 1) for two temperatures for a short-period FBG with Bragg wavelength in the 1550-nm telecom window. The grating was written by UV-laser in standard telecommunications single-mode fiber (SMF) with 125-μm cladding diameter.

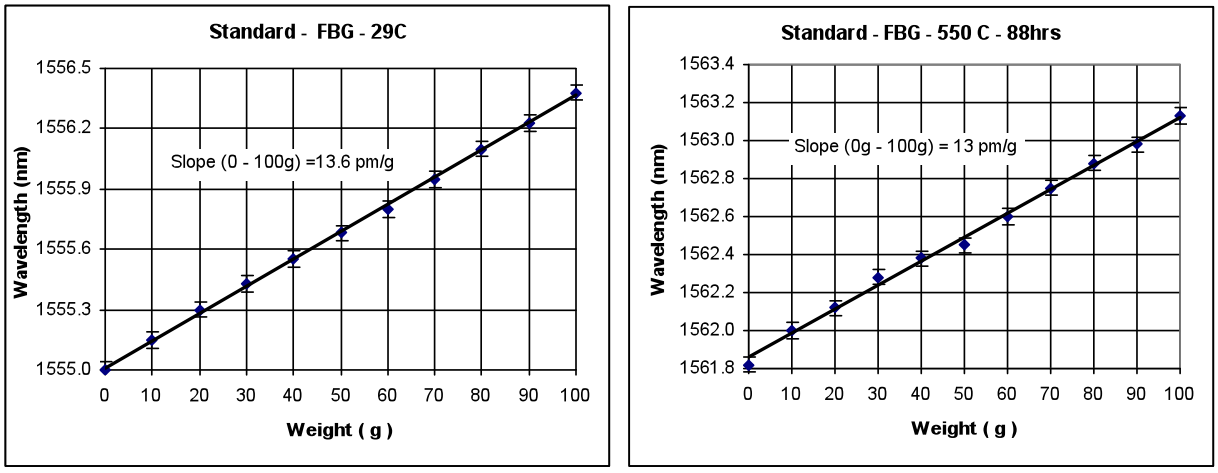

Figure 3. Standard FBG: Weight measurement (a) at 29°C, and (b) after 88 hours at 550°C (at which temperature the strain dependence was retained although the reflectivity decreased by 10 dB).

The plot on the left for near room temperature shows a wavelength shift of 13.6 pm per gram for Bragg wavelength of 1555 nm, i.e., a fractional wavelength shift of 8.74 ppm (parts-per-million). The plot on the right shows the same measurement performed at elevated temperature. The

grating had been held at 550°C for 88 hours. A similar wavelength shift was seen, 13 pm/gram. This wavelength shift corresponds to a fractional shift of 8.3 ppm of the elevated-temperature Bragg wavelength. Note that, for the unstretched fiber, the Bragg wavelength increased by 6.85 nm in going from 29°C to 550°C corresponding to 13.1 pm/°C. Thus, for this particular case the shift per gram and per degree Celsius are very similar. The oven used was subject to small air currents, and thus it was more difficult to keep the oven at as constant a temperature throughout the set of measurements as for the room temperature measurements.

4.2 Standard UV Written FBGs in 125-µm Two-Mode Optical Fiber near 1300 nm

The following plots show the Bragg wavelength shifts for angled (blazed) gratings written in two-mode fiber. The fiber used was AT&T Accutether-220 with cutoff around 1310 nm, thus allowing two bound modes around 1290 nm. The longer wavelength reflection corresponds to the usual reflection of the fundamental mode (i.e., conversion of the forward-propagating fundamental mode, often designated LP_{01}, into the backward propagating second mode, often designated LP_{11}). As seen in Figure 4(a), the Bragg wavelengths for both resonances ($LP_{01} \leftrightarrow LP_{01}$ labeled 01↔01 on the figure) and ($LP_{01} \leftrightarrow LP_{11}$ labeled 01↔11 on the figure) shift 5.5 nm with 500 grams, corresponding to 11 pm/gram around 1290 nm, i.e., a fractional wavelength shift of 8.5 ppm per gram.

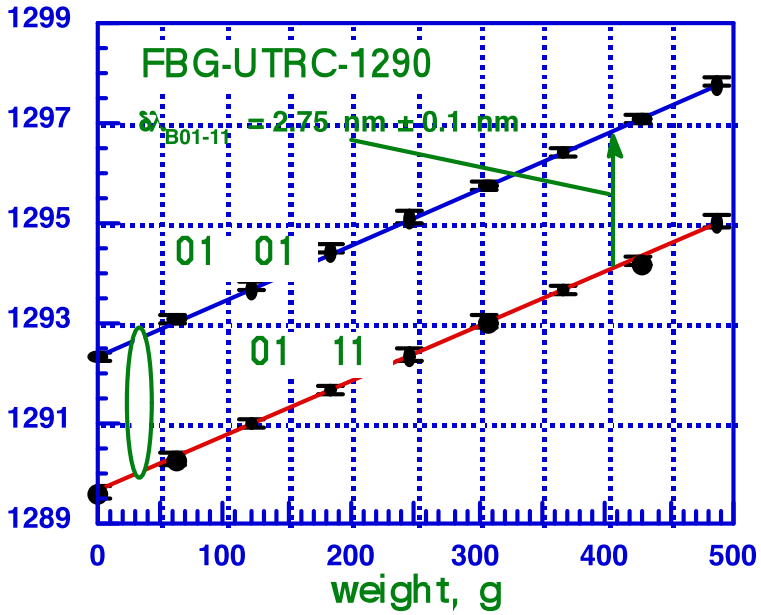

Figure 4. Two-mode fiber grating: Bragg resonance wavelengths as a function of weight applied to the fiber (producing a tension on the order of ≈1% per kg).

4.3 Chemical Composition Gratings in 115-µm Single-Mode Optical Fiber

In the following figures, we show results for chemical composition gratings written by ACREO with UV but with the fiber at an elevated temperature during writing as described in (3).

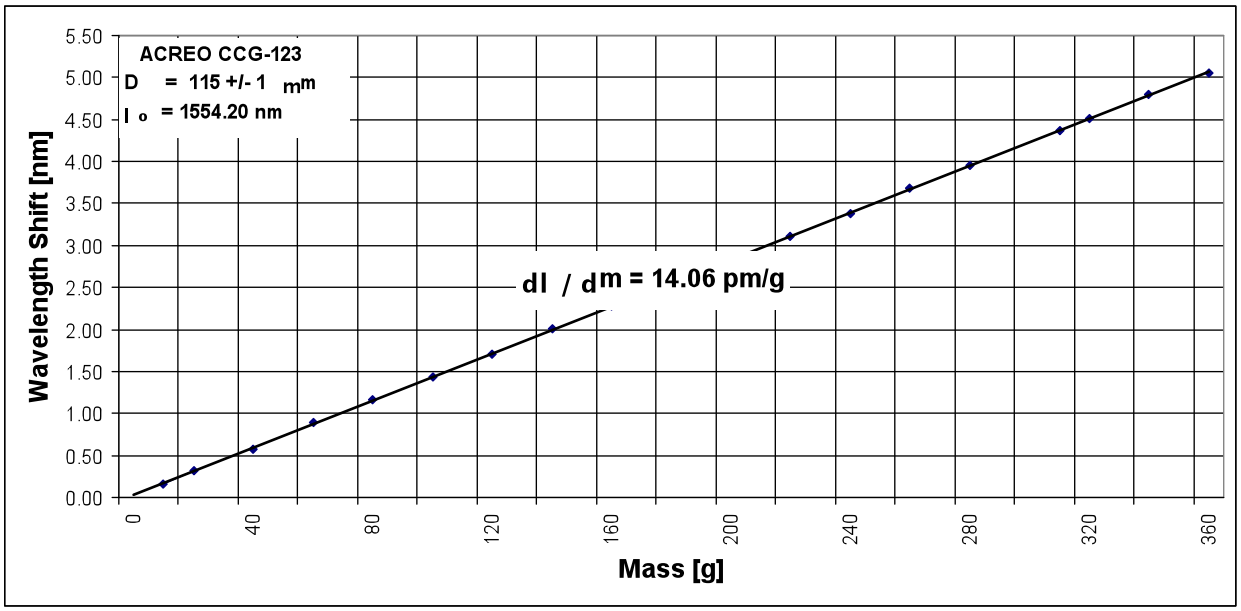

Figure 5. Weight measurement for chemical composition grating from ACREO with room temperature unstrained center wavelength 1554.2 nm.

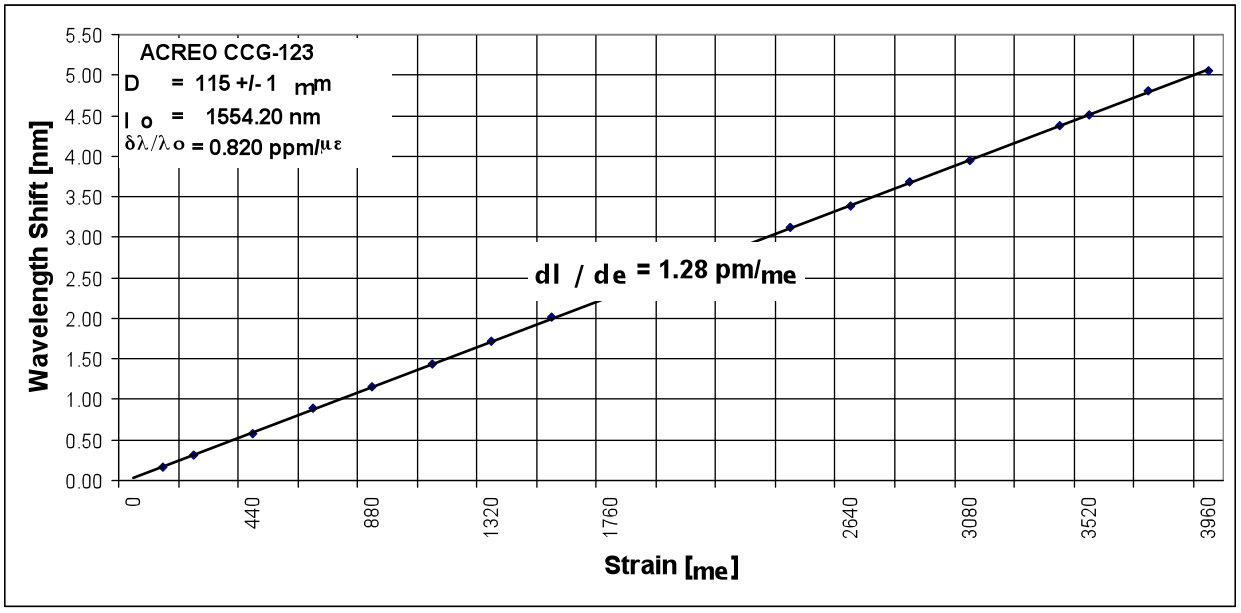

Figure 6. Gage factor deduced from weight measurement for ACREO grating.

4.4 Standard UV-Written Gratings in 80-µm Bend-Resistant Single-Mode Optical Fiber

In the following figures, we show results for UV-written gratings written in small cladding diameter (80-µm) bend-resistant optical fiber. As well as having a smaller cladding the core is smaller with a larger doping, higher Δ, to provide better bend-resistant guidance.

4.4.1 Weight Measurements and Deduced Results

The next two figures show the weight measurements for an array of 7 gratings in the 80-µm fiber. Weights were hung at the end of the grating array so that al gratings were subject to the same force. Figure 7 shows the spectra for each of the different weights used. All the peaks moved in unison as confirmed in Figure 8.

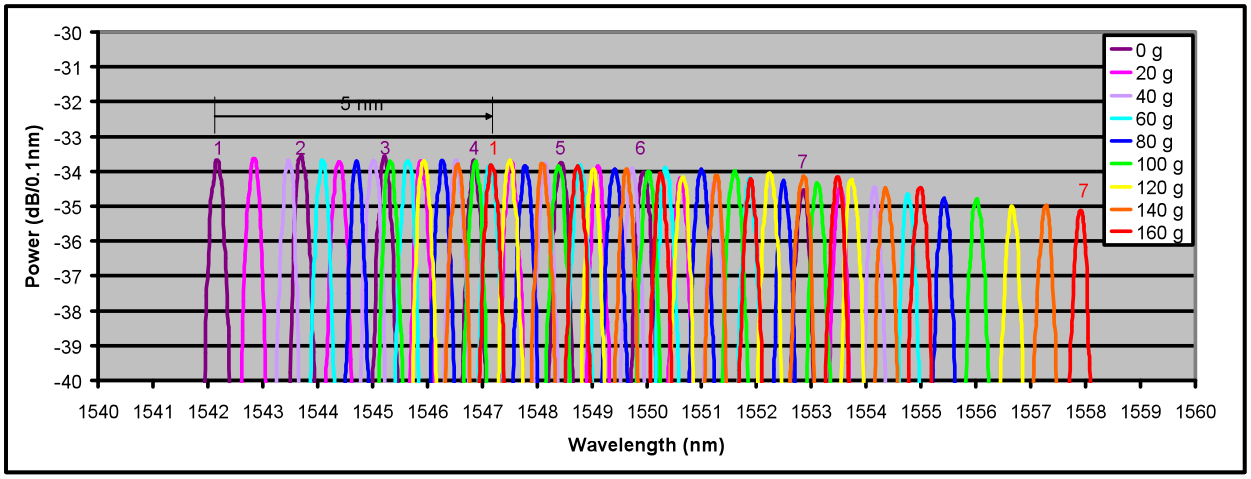

Figure 7. 7-grating array in 80-um bend-resistant optical fiber: Wavelength spectra for 9 different weights showing shift of approx. 5 nm when tension is applied by hanging 160 grams.

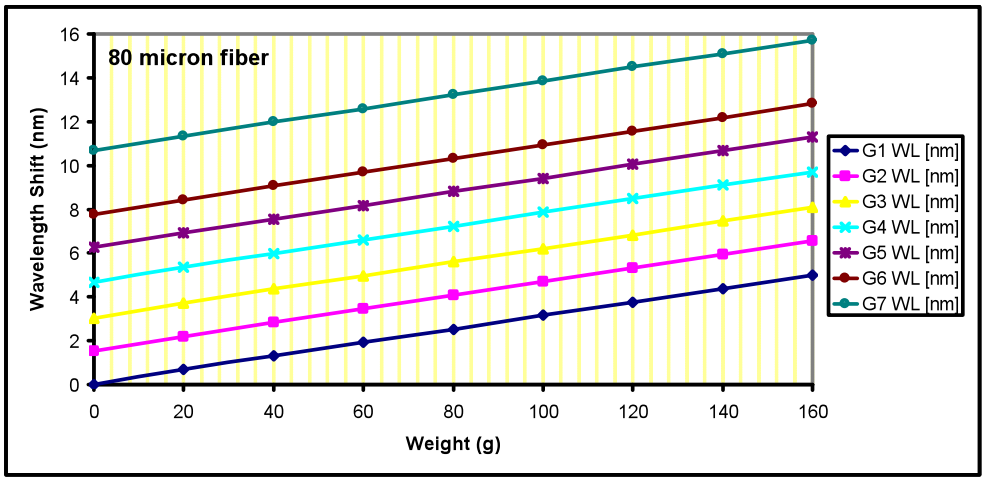

	Shift (pm/g)
G1	31.4
G2	31.2
G3	31.4
G4	31.4
G5	31.5
G6	31.4
G7	31.4
Av.	31.38

Figure 8. 7-Grating array in 80-um bend-resistant optical fiber: Wavelength shift versus weight for the Bragg wavelength peaks of the previous figure showing an average shift of 31.38 pm/gram and fractional shift 20.3 ppm/gram.

Figure 9 shows the wavelength shift as a function of strain deduced by assuming E_{silica} = 73 GPa and g = 9.81 ms^{-2}.

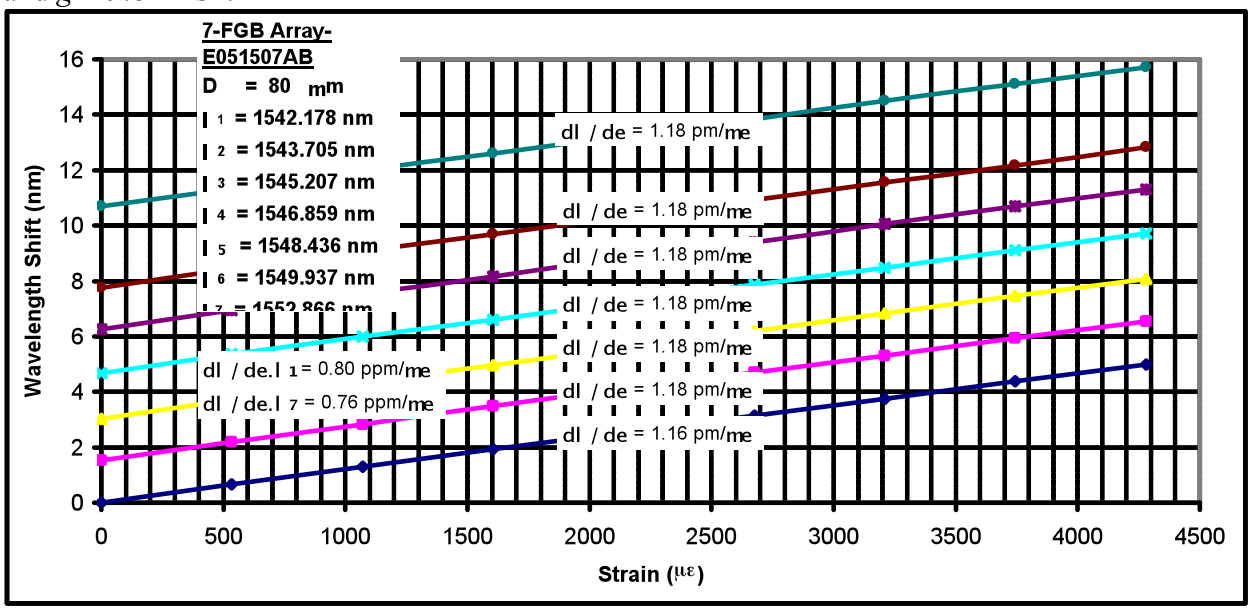

Figure 9. 7-Grating array in 80-□m bend-resistant optical fiber: Wavelength shift versus strain deduced by assuming E_{silica} = 73 GPa and g = 9.81 ms^{-2}.

4.4.2 Stretching Measurements

The following figures show stretching measurements (performed as described in Section 3.2) for a 4-grating array in the 80-μm bend-resistant optical fiber. Figure 10 shows the wavelength spectra shifting to longer wavelengths as the grating array is stretched in successive increments. The actual wavelengths versus elongation are plotted in Figure 11 together with the fractional wavelength shift (in parts-per-million) versus strain (in microstrain).

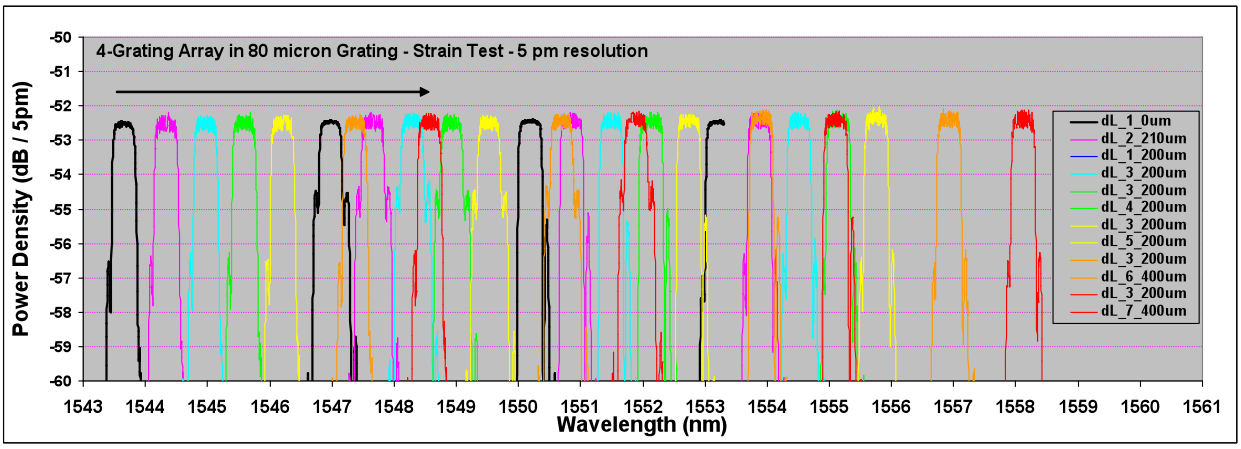

Figure 10. 4-grating array in 80-□m bend-resistant optical fiber: Wavelength spectra seen increasing in wavelength as the grating array is stretched in increments given in the legend.

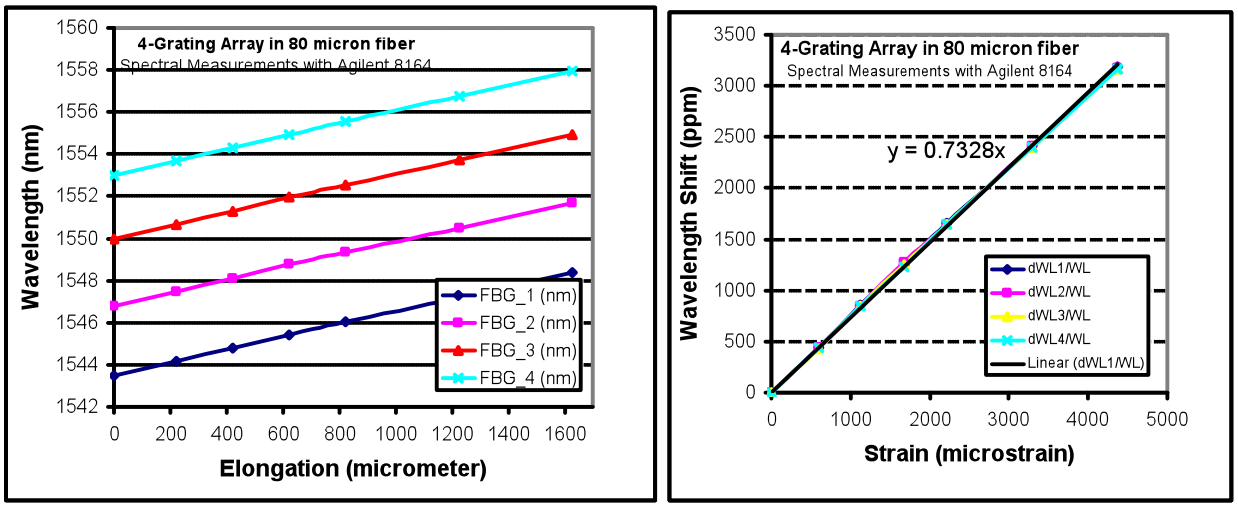

Figure 11. 4-Grating array in 80-um bend-resistant optical fiber: (a) Wavelength shift versus elongation given a separation between clamp points of 371.5 mm. (b) Fractional wavelength shift versus fractional elongation (strain).

4.5 Modal Interferometric Long-Period Gratings

The following figure shows weight measurements (performed as described in Section 3.1) for long-period "modal interferometric" grating fabricated point-by-point with an electric arc as described in (4). We note that the temperature dependence is much less than for the standard FBGs. On the other hand the strain gage factor is over an order of magnitude larger.

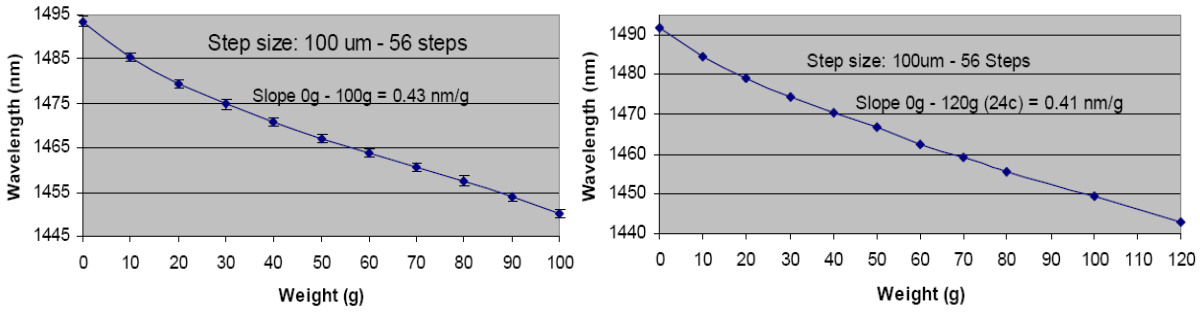

Figure 12. IFOS fabricated electric-arc-written Long-Period Grating (LPG): Weight measurements at (a) room temperature, and (b) at 650°C after being held at that temperature for 32 hours.

5. SUMMARY AND CONCLUSIONS

In conclusion, Fiber Bragg Gratings (FBGs) can act as highly-accurate, multiplexable, EMI-immune strain gages. We have provided experimental and theoretical results showing how their

gage factor can vary for a range of optical fiber and grating types. Table 2 provides a summary of results. For short period gratings (SPGs), while the wavelength shift per unit mass of the weights hung on the fiber, $\delta\lambda/\delta m$, is inversely proportional to the fiber diameter, the wavelength shift per unit strain remains of order 1.2 pm/gram. On the other hand for "modal interferometric" long-period gratings that IFOS has fabricated, we have found an increase in the strain gage factor by over an order of magnitude and, at the same time a decrease in the temperature dependence.

Table 2. Summary of Measurement Results

Case/ Sec.	Fiber Diameter (μm)	Grating Form	Grating Writing	λ_o [nm]	$\delta\lambda/\delta m$ [pm/g]	$(\delta\lambda/\lambda)/\delta m$ [ppm/g]	$\delta\lambda/\delta\varepsilon$ [pm/με]	$(\delta\lambda/\lambda)/(\delta l/l)$ [ppm/με]
Liter-ature	125	SPG, SMF		1550	13.3(D)	8.57(D)	1.21	0.78**
4.1	125	SPG, SMF	Standard UV	1555.34	13.6	8.74	1.24 (D)	0.79 (D)
4.2	125	SPG, TMF	Standard UV, Angled	1290	11.0	8.53	1.00 (D)	0.78 (D)
4.3	115	SPG, SMF	CCG UV	1554.2	14.06	9.05	1.28 (D)	0.72 (D)
4.4.1	80	SPG, SMF	Standard UV	1542-1550	31.38	20.3	1.18 (D)	0.76 (D)
4.4.2	80	SPG, SMF	Standard UV	1542-1550	31.38	20.3	1.13 (M)	0.73 (M)
4.5	125	MI-LPG< SMF	Electric Arc	1490	-430	-289	-39.1 (D)	-26.2 (D)

*M indicates directly measured; D indicates deduced assuming Young's Modulus E_{silica} = 73 GPa and g = 9.81 m.s^{-2}.**0.78 = (1 - Photoelastic coefficient for pure fused silica)

6. ACKNOWLEDGEMENTS

We thank Dr. Ken Fesler, formerly of IFOS, now of Agilent, for initial development of the "hanging weights" measurement method, Dr. Bill Morey, formerly of UTRC, for providing the two-mode fiber grating (Sec. 4.2), Dr. Carola Sterner of ACREO for providing the chemical composition grating (Sec. 4.3), and Mr. Keo Sourichanh, formerly of IFOS, for fabricating and performing measurements on the electric arc written grating (Sec. 4.5). The measurements for the different gratings were performed as part of projects funded by the Air Force (Phase II SBIR Contract FA8650-06-C-5207) as well as the National Science Foundation (NSF) (Phase I SBIR Award III-9360932) and NASA (Phase-II SBIR Contract NNJ06JA36C).

7. REFERENCES

1. F.-K. Chang, *Structural Health Monitoring, DEStech* Publications, Inc., Lancaster, PA, 2007.
2. R.J. Black and B. Moslehi, "Fiber Bragg Grating Interrogators for Structural Health Monitoring", Abstract accepted for *SAMPE '08*, Long Beach, CA May 18-22, 2008. Paper ID L319.
3. A. T. Alavie, S.E. Karr, A. Othonos, and R.M. Measures, "A multiplexed Bragg grating fiber laser sensor system", *IEEE Photonics Technol. Lett.* **5** (9), 1112-4 (1993).
4. Y.-J. Chiang, L. Wang, H.-S. Chen, C.-C. Yang, and W.-F. Liu, "Multipoint Temperature-Independent Fiber-Bragg-Grating Strain-Sensing System Employing an Optical-Power-Detection Scheme," *Appl. Opt*. **41**, 1661-7 (2002).
5. M. Fokine, "Formation of thermally stable chemical composition gratings in optical fibers," *J. Opt. Soc. Am. B* **19**, 1759-1765 (2002).
6. R. J. Black, K. Chau, G. Chen, B. Moslehi, L. Oblea, and K. Sourichanh, "Optical fiber gratings for structural health monitoring in high-temperature environments", *SPIE Sensor Systems and Networks: Phenomena, Technology, and Applications for NDE and Health Monitoring* 2007.
7. http://www.sciner.com/Opticsland/FS.htm gives E_{silica} = 73 GPa at 25 °C.
8. R. G. Munro, *Elastic Moduli Data for Polycrystalline Ceramics*, *NIST Property Data Summaries, NISTIR* **6853**, (2002), National Institute of Standards and Technology, Gaithersburg, Maryland 20899 – http://www.ceramics.nist.gov/srd/summary/SiO2.htm - gives a value E_{silica} = 73.06 GPa.
9. Ed Friedman and J.L. Miller, Photonics Rules of Thumb, 2nd ed., SPIE, McGraw-Hill, 2003 – Table A.19 give E_{silica} = 74.5 GPa.
10. http://www.allmeasures.com/formulae/static/materials/157/youngs_modulus.htm gives E_{silica} = 94 GPa.